

Published in final edited form as:

*Nature*. 2005 December 22; 438(7071): 1162–1166. doi:10.1038/nature04302.

## NMDA receptors are expressed in oligodendrocytes and activated in ischaemia

Ragnhildur Káradóttir, Pauline Cavelier, Linda H. Bergersen, and David Attwell

Department of Physiology, University College London, Gower Street, London, WC1E 6BT, England  
Department of Anatomy and Centre for Molecular Biology and Neuroscience, University of Oslo, PO Box 1105, Blindern, N-0317 Oslo, Norway

### Abstract

Glutamate-mediated damage to oligodendrocytes contributes to mental or physical impairment in periventricular leukomalacia (pre- or perinatal white matter injury leading to cerebral palsy), spinal cord injury, multiple sclerosis and stroke<sup>1–4</sup>. Unlike neurons<sup>5</sup>, white matter oligodendrocytes reportedly lack NMDA receptors<sup>6,7</sup> and it is believed that glutamate damages oligodendrocytes, especially their precursor cells, by acting only on calcium-permeable AMPA/kainate receptors<sup>1–4</sup> or by reversing cystine-glutamate exchange and depriving cells of antioxidant protection<sup>8</sup>. We now show that precursor, immature and mature oligodendrocytes in the white matter of the cerebellum and corpus callosum exhibit NMDA evoked currents, mediated by receptors which are blocked only weakly by Mg<sup>2+</sup>, which may contain NR1, NR2C and NR3 subunits. NMDA receptors are present in the myelinating processes of oligodendrocytes, where the small intracellular space could lead to a large rise of intracellular ion concentration in response to NMDA receptor activation. Simulating ischaemia led to an inward current developing in oligodendrocytes, which was partly mediated by NMDA receptors. These results point to NMDA receptors of unusual subunit composition as a novel therapeutic target for preventing white matter damage in a range of diseases.

---

Blocking AMPA/kainate receptors attenuates white matter injury in animal models of hypoxia/ischaemia<sup>9,10</sup>, spinal cord injury<sup>11,12</sup> and multiple sclerosis<sup>13,14</sup>. Nevertheless, NMDA receptors were found in some cultured oligodendrocyte precursors<sup>15</sup> and in spinal grey (but not white) matter oligodendrocytes<sup>16</sup>, and NMDA receptor blockers slow the loss of white matter action potentials<sup>10</sup> and reduce white matter damage in ischaemia<sup>17</sup> and in a model of multiple sclerosis<sup>18</sup>. We have, therefore, re-examined the involvement of NMDA receptors in the physiology and pathology of oligodendrocytes.

Whole-cell clamped precursor, immature and mature oligodendrocytes in the white matter could be distinguished by their morphology and antibody labelling<sup>7,19</sup> (Fig. 1a–c). Precursor cells (Fig. 1a) had short processes not aligned with nearby axons, were labelled by antibodies to NG2 proteoglycan (for the specificity of this, see Methods), and often exhibited spontaneous synaptic currents (as in grey matter oligodendrocytes<sup>20</sup>) which were blocked by TTX (Fig. 1d). Immature cells (Fig. 1b) had some processes aligned with adjacent axons, and were labelled by antibody to O4 lipid sulfate. Mature cells (Fig. 1c) had most processes aligned with axons, and were labelled by antibody to myelin basic protein (MBP). Oligodendrocyte membrane resistance decreased with maturity (Fig. 1e). The resting potential was approximately  $-60\text{mV}$  ( $-57.5 \pm 2.9\text{mV}$  in 37 mature cells: without shunting by the electrode seal it would be  $\sim 4\text{mV}$  more negative).

Precursor, immature and mature cerebellar white matter oligodendrocytes responded to glutamate (100 $\mu$ M) with an inward current at  $-63$ mV, which was unaffected by 1 $\mu$ M TTX ( $p=0.4$ ; Fig. 1f–h, Supplementary Fig. 1), showing that axonal action potentials generated by glutamate depolarizing neurons did not contribute to the current (e.g. by releasing  $K^+$ ). The current was potentiated when the local glutamate concentration was raised by blocking glutamate transporters with TBOA ( $p=0.016$ ; Fig. 1g, Supplementary Fig 1). D-AP5, MK-801 and NBQX all reduced the glutamate-evoked current (Fig. 1h,i), suggesting the presence of both NMDA and AMPA/kainate receptors.

NMDA (60 $\mu$ M) evoked an inward current in corpus callosum (Fig. 2a–c) and cerebellum (Fig. 2d,e) oligodendrocytes, which was comparable in size (at  $-63$ mV in 0mM  $Mg^{2+}$ ) to the current produced by AMPA (20 $\mu$ M) or kainate (30 $\mu$ M), and was larger than that produced by the metabotropic glutamate receptor agonist (1S,3R)-ACPD (100 $\mu$ M). In cerebellar oligodendrocytes the NMDA-evoked current was largest in mature cells (Fig. 2f,  $p=0.042$  compared with precursors) although the increased membrane area of mature cells may imply a lower current density. The NMDA-evoked current ran down slightly with time (Fig. 2g), so the current in drugs was quantified relative to the average of preceding and following control responses. It was blocked by D-AP5 (Fig. 2h,j) and unaffected by TTX, NBQX, strychnine or bicuculline (Fig. 2i,j), and not significantly affected ( $p=0.072$ ) when glycine (100 $\mu$ M, with strychnine 5 $\mu$ M) was present, implying that the NMDA receptors' glycine-binding sites are well activated by endogenous glycine or D-serine. Changing from  $Mg^{2+}$ -free superfusion solution to solution containing 2mM  $Mg^{2+}$  decreased the NMDA-evoked current at  $-63$ mV 3 to 5-fold, independent of developmental age (Fig. 2k,l). This decrease is much less than is found for most neurons<sup>21</sup>, or for most cloned NMDA receptors<sup>22</sup>, which show a 60-fold reduction for receptors comprising NR1 and NR2A or 2B subunits and a 20-fold reduction for receptors comprising NR1 and NR2C or 2D subunits, but is comparable to that seen for cloned receptors comprising NR1, NR2A and NR3A subunits<sup>23</sup>.

Ifenprodil (10 $\mu$ M), which blocks NR2B-containing receptors, had no effect on the NMDA-evoked current (Fig. 2j). Neither pregnenolone sulphate (100 $\mu$ M, which potentiates NR1/NR2A and NR1/NR2B receptors by 60–82% but inhibits NR1/NR2C and NR1/NR2D receptors by 32%), nor D-cycloserine (1mM, with no added glycine, which potentiates NR1/NR2C receptors but inhibits NR1/NR2A and NR1/NR2B receptors), nor D-serine (100 $\mu$ M, with no glycine, which potentiates receptors lacking NR3 subunits but inhibits NR3-containing receptors) affected the current (Fig. 2j). This suggests the presence of a subunit (perhaps NR3) which suppresses modulatory actions on NR2 subunits, or the presence of a combination of subunits that these agents modulate in opposite directions (e.g. NR1/NR2A/NR2C or NR1/NR2/NR3), or a mix of receptors with different subunit combinations. Although the subunit composition currently remains uncertain, it allows these receptors to generate a significant current even at the resting potential in physiological [ $Mg^{2+}$ ].

In precursor oligodendrocytes the NMDA-evoked current reversed around 0mV (Fig 2m), and in 2mM  $Mg^{2+}$  the I-V relation showed a region of negative slope which was similar to, but less marked than, that produced by  $Mg^{2+}$ -block of neuronal NMDA receptor channels. In mature oligodendrocytes the I-V relation often failed to reverse at positive potentials, which may reflect the NMDA receptors being electrotonically distant from the soma in the cell processes (see below), or NMDA receptor activation leading to  $Na^+$  entry and block of a  $K^+$  current in the cell<sup>24</sup>.

Antibodies to NMDA receptor subunits labelled the myelinating processes, and some cell bodies, of oligodendrocytes in the cerebellar white matter. Labelling for NR2C (Fig. 3a,b) was abolished by omitting the primary antibody, or by preabsorption with the peptide to

which it was raised (Supplementary Fig. 2). Labelling was also seen for NR1 subunits, which colocalized with MBP in mature cells (data not shown), and NR3 subunits (Fig 3c,d, Supplementary Fig 2). Weaker labelling was seen for NR2A, NR2B and NR2D, and was abolished by omitting the primary antibody (NR2A, NR2B and NR2D) or by peptide absorption (NR2D). Double labelling showed colocalization of NR3 and NR2C subunits, and of NR1 and NR2C subunits in oligodendrocyte processes (Supplementary Figs. 3 & 4). These data, the lack of ifenprodil block, and the weak  $Mg^{2+}$ -block of the NMDA-evoked current, suggest that oligodendrocyte NMDA receptors contain at least NR1, NR2C and NR3 subunits.

Post-embedding electron microscopic immunocytochemistry showed that NR1 subunits were present in the myelinating processes of adult cerebellar oligodendrocytes (Fig. 3e,f, Supplementary Fig. 5), in the outer- and innermost membranes and also within the myelin (perhaps remaining from earlier in development). By quantifying the immunogold particles in the myelin and in the postsynaptic densities of mossy fibre-granule cell (Supplementary Fig. 5) and parallel fibre-Purkinje cell synapses, we found that the density of NMDA receptors throughout the myelin is as high as at the mossy fibre to granule cell synapse (Fig. 3g). The density of particles in the outer membrane of the myelin (where the receptors may sense glutamate released from surrounding cells) tended ( $p=0.064$ ) to be larger than that in the innermost membrane (where the receptors may sense glutamate released from the axon), but both were similar to the average density measured over all of the myelin ( $36.4\pm 8.3$ ,  $17.7\pm 4.3$  and  $33.6\pm 4.5$  particles/ $\mu m^2$  respectively).

To examine the role of oligodendrocyte NMDA receptors in pathological situations, we simulated the energy deprivation which contributes to periventricular leukomalacia, or occurs after ischaemia in spinal cord injury. Simulated ischaemia solution evoked a slowly developing inward current in precursor and mature oligodendrocytes (Fig. 4, peak inward current at  $-63mV$  after  $\sim 7$  mins was  $307\pm 83$  and  $280\pm 48$  pA in 7 precursor and 8 mature cells in  $2mM Mg^{2+}$ ). This current was generated partly by a rise of extracellular [glutamate], since it was reduced by D-AP5 and NBQX (Fig. 4a). In some precursors (Fig. 4a,c) the inward current early in ischaemia included an increased frequency of synaptic current-like events (Fig. 1d), presumably reflecting exocytotic transmitter release triggered by action potentials or a rise of axonal  $[Ca^{2+}]_i$ . The relative contribution of NMDA and AMPA receptors to the glutamate-mediated current was analysed in  $0mM Mg^{2+}$  to detect NMDA receptor currents more accurately (in  $2mM Mg^{2+}$  the NMDA component at  $-63mV$  would be 4-fold smaller (Fig. 2l), but would be increased in unclamped cells by the ischaemia-evoked current depolarizing cells and reducing NMDA receptor  $Mg^{2+}$ -block). The NMDA receptor mediated current in precursors was on average 50% larger than that mediated by AMPA/kainate receptors (Fig 4b–d), and in some cells comprised almost all the current (Fig. 4c). In mature oligodendrocytes the fraction of the inward current that was generated by glutamate was smaller than in precursors (Fig. 4d), suggesting that (since mature cells can generate larger glutamate and NMDA-evoked currents: Figs. 1f, 2f) less glutamate release occurs around mature cells in ischaemia. Further work is needed to establish the origin of the part of the inward current that is not generated by glutamate release.

We have shown that oligodendrocytes express functional NMDA receptors. The NMDA-evoked currents that we observe are unlikely to be produced by an agent released secondarily from neurons because they are unaffected by TTX, or by block of AMPA/KA, mGluR, GABA<sub>A</sub>, or glycine receptors (Figs. 2j, 1i) and oligodendrocytes show no current in response to application of noradrenaline, dopamine, histamine, 5-HT, ATP, adenosine or ACh (data not shown). Antibody labelling (Fig. 3) and the voltage-dependence of the current (Fig 2m) show that oligodendrocytes themselves express NMDA receptors. Previous work which failed to detect NMDA receptor currents in oligodendrocytes was partly on cultured

cells<sup>6</sup>, which may down-regulate their NMDA receptor expression. Our data (Fig. 2a) contradict the absence of NMDA responses reported in corpus callosum oligodendrocytes<sup>7</sup>. Since oligodendrocyte NMDA receptor currents occur both in cerebellum and corpus callosum (Fig. 2), they may represent a general property of white matter oligodendrocytes. Our electrophysiological recordings are from precursor, immature and mature oligodendrocytes in P7-P14 rats, and remain to be extended to the adult, but NMDA receptor subunits are also present in adult oligodendrocytes (Fig. 3e).

Oligodendrocyte NMDA receptors are likely to play a role in controlling oligodendrocyte development and myelination<sup>26</sup>, and in damaging these cells in pathological conditions. They show only weak  $Mg^{2+}$ -block at the cells' resting potential (Fig. 2l)<sup>16</sup>, and mediate part of the inward current generated in oligodendrocytes in response to simulation of the energy deprivation which occurs in periventricular leukomalacia, in stroke, and after ischaemia in spinal cord injury. Notably, they are present in the oligodendrocytes' myelinating processes, where the intracellular volume is small and receptor-mediated ion influx may produce a large intracellular concentration rise and osmotic water flux which could disrupt myelination. The higher glutamate affinity of NMDA receptors, relative to AMPA receptors, makes them more likely to be activated in neurodegenerative disorders which involve a prolonged but small rise of extracellular glutamate concentration, as may occur in multiple sclerosis. Thus, oligodendrocyte NMDA receptors could contribute to causing the white matter damage which occurs when the extracellular [glutamate] is raised in periventricular leukomalacia, spinal cord injury, multiple sclerosis and stroke<sup>1–4</sup>. Indeed, in the optic nerve, activation of NMDA receptors on oligodendrocyte processes, when glutamate is released during ischaemia, leads to the disintegration of those processes<sup>27</sup>. The unusual subunit combination of these receptors, which may contain NR1, NR2C and NR3 subunits, suggests they may be a useful therapeutic target in a variety of brain disorders.

## Methods

### Brain slices

Cerebellar or forebrain slices (225 $\mu$ m thick) were prepared from P7-P14 rats in solution containing 1mM Na-kynureate to block glutamate receptors. Cerebellum myelinates relatively late, facilitating investigation of different developmental stages, and corpus callosum is an area which is thinned in severe periventricular leukomalacia. Slices were superfused at 33 $\pm$ 1 $^{\circ}$ C with bicarbonate-buffered solution (for ischaemia) or at 24 $\pm$ 1 $^{\circ}$ C with HEPES-buffered solution (for non-ischaemia experiments), containing (mM) 126 NaCl, 24 NaHCO<sub>3</sub>, 1 NaH<sub>2</sub>PO<sub>4</sub>, 2.5 KCl, 2 MgCl<sub>2</sub>, 2.5 CaCl<sub>2</sub>, 10 glucose, 0.1 glycine (activates the NMDA receptor glycine site), strychnine 0.005 (blocks glycine receptors), bubbled with 95% O<sub>2</sub>/5% CO<sub>2</sub>, pH 7.4; or 144 NaCl, 2.5 KCl, 2 MgCl<sub>2</sub>, 10 HEPES, 1 NaH<sub>2</sub>PO<sub>4</sub>, 2.5 CaCl<sub>2</sub>, 10 glucose, 0.1 glycine, strychnine 0.005, pH set to 7.4 with NaOH. Omitting glycine or adding D-serine did not affect the NMDA receptor current (see text). To simulate ischaemia we replaced external O<sub>2</sub> by N<sub>2</sub>, and external glucose by 7mM sucrose, added 2mM iodoacetate to block glycolysis, and added 100 $\mu$ M rotenone or 25 $\mu$ M antimycin to block oxidative phosphorylation<sup>25</sup>. Without iodoacetate and rotenone/antimycin, it took ~3-fold longer for the ischaemia-evoked inward current to develop, probably because in an open chamber O<sub>2</sub> can diffuse to the slice allowing glycogen metabolism in mitochondria for longer than would occur in vivo<sup>25</sup>.

### Recording & cell identification

White matter cells (avoiding cerebellar nuclei) were whole-cell clamped with pipettes containing a K<sup>+</sup>-based solution (for glutamate application) comprising (mM) 130 KCl, 4 NaCl, 0.5 CaCl<sub>2</sub>, 10 HEPES, 10 EGTA, 2 MgATP, 0.5 Na<sub>2</sub>GTP, K-Lucifer yellow 2, pH set

to 7.2 with KOH, or a Cs<sup>+</sup>-based solution (for NMDA application and ischaemia), comprising (mM) 130 CsCl, 4 NaCl, 0.5 CaCl<sub>2</sub>, 10 HEPES, 10 BAPTA, 2 MgATP, 0.5 Na<sub>2</sub>GTP, K-Lucifer yellow 2, pH set to 7.2 with CsOH. Series resistance was 8–20MΩ, before 60% compensation. Cells were identified from post-recording dye-fill morphology and antibody labelling. NG2 antibody labelled 15 out of 15 tested cells with precursor morphology (we take NG2 labelling to indicate oligodendrocyte precursors<sup>20</sup>, however some NG2 cells may be a glial class distinct from oligodendrocytes<sup>28</sup>, or (in grey matter) neuronal precursors<sup>29</sup>; demonstrating that oligodendrocytes express NMDA receptors does not depend on recording precursors, since NMDA receptor currents were also seen in immature and mature cells). O4 antibody labelled 6 out of 6 cells with immature morphology. MBP antibody labelled all 17 cells tested with mature morphology. Antibody to the oligodendrocyte transcription factor Olig2 labelled all 10 cells tested (7 precursors, 1 immature and 2 mature cells). Oligodendrocytes could be distinguished from astrocytes, which showed gap junction coupling, revealed by Lucifer yellow spreading to other cells, and GFAP labelling (5 out of 5 cells). Electrode junction potentials were compensated. I-V relations were from responses to 200 msec voltage steps.

### Immunocytochemistry

Antibody labelling and post-embedding electron microscopic immunocytochemistry are described in Supplementary Material.

### Statistics

Data are mean ± s.e.m. P values are from Student's 2-tailed t-tests, except for multiple comparisons done with one-way Anova and Tukey post hoc test.

### Supplementary Material

Refer to Web version on PubMed Central for supplementary material.

### Acknowledgments

We thank D. Rowitch, C.D. Stiles & J. Alberta for Olig2 antibody, F.A. Stephenson, R.J. Wenthold & O.P. Ottersen for NR1 antibody, and A. Gibb, K. Jessen, R. Mirsky, W. Richardson, D. Rossi, J. Rothman, A. Silver & J. Storm-Mathisen for advice. Supported by the Wellcome Trust, EU, Norwegian Research Council & a Wolfson-Royal Society Award. R. Káradóttir was in the 4 year PhD Programme in Neuroscience at UCL.

### References

1. Volpe JJ. Neurobiology of periventricular leukomalacia in the premature infant. *Pediatr Res.* 2001; 50:553–562. [PubMed: 11641446]
2. Stys PK. White matter injury mechanisms. *Curr Mol Med.* 2004; 4:113–130. [PubMed: 15032708]
3. Matute C, Alberdi E, Domercq M, Perez-Cerda F, Perez-Samartin A, Sanchez-Gomez MV. The link between excitotoxic oligodendroglial death and demyelinating diseases. *Trends Neurosci.* 2001; 24:224–230. [PubMed: 11250007]
4. Dewar D, Underhill SM, Goldberg MP. Oligodendrocytes and ischemic brain injury. *J Cereb Blood Flow Metab.* 2003; 23:263–274. [PubMed: 12621301]
5. Choi DW. Glutamate neurotoxicity and diseases of the nervous system. *Neuron.* 1988; 1:623–634. [PubMed: 2908446]
6. Patneau DK, Wright PW, Winters C, Mayer ML, Gallo V. Glial cells of the oligodendrocyte lineage express both kainate- and AMPA-preferring subtypes of glutamate receptor. *Neuron.* 1994; 12:357–371. [PubMed: 7509160]
7. Berger T, Walz W, Schnitzer J, Kettenmann H. GABA- and glutamate-activated currents in glial cells of the mouse corpus callosum slice. *J Neurosci Res.* 1992; 31:21–27. [PubMed: 1351952]



8. Oka A, Belliveau MJ, Rosenberg PA, Volpe JJ. Vulnerability of oligodendroglia to glutamate: pharmacology, mechanisms, and prevention. *J Neurosci.* 1993; 13:1441–1453. [PubMed: 8096541]
9. Follett PL, Rosenberg PA, Volpe JJ, Jensen FE. NBQX attenuates excitotoxic injury in developing white matter. *J Neurosci.* 2000; 20:9235–9241. [PubMed: 11125001]
10. Tekkök SB, Goldberg MP. AMPA/kainate receptor activation mediates hypoxic oligodendrocyte death and axonal injury in cerebral white matter. *J Neurosci.* 2001; 21:4237–4248. [PubMed: 11404409]
11. Agrawal SK, Fehlings MG. Role of NMDA and non-NMDA ionotropic glutamate receptors in traumatic spinal cord axonal injury. *J Neurosci.* 1997; 17:1055–1063. [PubMed: 8994060]
12. Wrathall JR, Teng YD, Marriott R. Delayed antagonism of AMPA/kainate receptors reduces long-term functional deficits resulting from spinal cord trauma. *Exp Neurol.* 1997; 145:565–573. [PubMed: 9217092]
13. Pitt D, Werner P, Raine CS. Glutamate excitotoxicity in a model of multiple sclerosis. *Nature Medicine.* 2000; 6:67–70.
14. Smith T, Groom A, Zhu B, Turski L. Autoimmune encephalomyelitis ameliorated by AMPA antagonists. *Nature Medicine.* 2000; 6:62–66.
15. Wang C, Pralong WF, Schulz MF, Rougon G, Aubry JM, Pagliusi S, Robert A, Kiss JZ. Functional N-methyl-D-aspartate receptors in O-2A glial precursor cells: a critical role in regulating polysialic acid-neural cell adhesion molecule expression and cell migration. *J Cell Biol.* 1996; 135:1565–1581. [PubMed: 8978823]
16. Ziak D, Chvatal A, Sykova E. Glutamate, kainate and NMDA-evoked membrane currents in identified glial cells in rat spinal cord slice. *Physiol Res.* 1998; 47:365–375. [PubMed: 10052606]
17. Schäbitz WR, Li F, Fisher M. The N-methyl-D-aspartate antagonist CNS 1102 protects cerebral gray and white matter from ischemic injury following temporary focal ischemia in rats. *Stroke.* 2000; 31:1709–1714. [PubMed: 10884477]
18. Wallström E, Diener P, Ljungdahl A, Khademi M, Nilsson CG, Olsson T. Memantine abrogates neurological deficits, but not CNS inflammation, in Lewis rat experimental autoimmune encephalomyelitis. *J Neurol Sci.* 1996; 137:89–96. [PubMed: 8782160]
19. Back SA, Luo NL, Borenstein NS, Levine JM, Volpe JJ, Kinney HC. Late oligodendrocyte progenitors coincide with the developmental window of vulnerability for human perinatal white matter injury. *J Neurosci.* 2001; 21:1302–1312. [PubMed: 11160401]
20. Bergles DE, Roberts JDB, Somogyi P, Jahr CE. Glutamatergic synapses on oligodendrocyte precursor cells in the hippocampus. *Nature.* 2000; 405:187–191. [PubMed: 10821275]
21. Kirson ED, Schirra C, Konnerth A, Yaari Y. Early postnatal switch in magnesium sensitivity of NMDA receptors in rat CA1 pyramidal cells. *J Physiol.* 1999; 521:99–111. [PubMed: 10562337]
22. Kuner T, Schoepfer R. Multiple structural elements determine subunit specificity of Mg<sup>2+</sup> block in NMDA receptor channels. *J Neurosci.* 1996; 16:3549–3558. [PubMed: 8642401]
23. Sasaki YF, et al. Characterization and comparison of the NR3A subunit of the NMDA receptor in recombinant systems and primary cortical neurons. *J Neurophysiol.* 2002; 87:2052–2063. [PubMed: 11929923]
24. Borges K, Kettenmann H. Blockade of K<sup>+</sup> channels induced by AMPA/kainate receptor activation in mouse oligodendrocyte precursor cells is mediated by Na<sup>+</sup> entry. *J Neurosci Res.* 1995; 42:579–593. [PubMed: 8568944]
25. Allen NJ, Káradóttir R, Attwell D. A preferential role for glycolysis in preventing the anoxic depolarization of rat hippocampal area CA1 pyramidal cells. *J Neurosci.* 2005; 25:848–859. [PubMed: 15673665]
26. Yuan X, Eisen AM, McBain CJ, Gallo V. A role for glutamate and its receptors in the regulation of oligodendrocyte development in cerebellar tissue slices. *Development.* 1998; 125:2901–2914. [PubMed: 9655812]
27. Salter, M. & Fern, R. NMDA receptors are expressed in developing oligodendrocyte processes and mediate injury. (2005). Submitted.
28. Berry M, Hubbard P, Butt AM. Cytology and lineage of NG2-positive glia. *J Neurocytol.* 2002; 31:457–467. [PubMed: 14501216]

29. Chittajulu R, Aguirre A, Gallo V. NG2-positive cells in the mouse white and grey matter display distinct physiological properties. *J Physiol.* 2004; 561:109–122. [PubMed: 15358811]

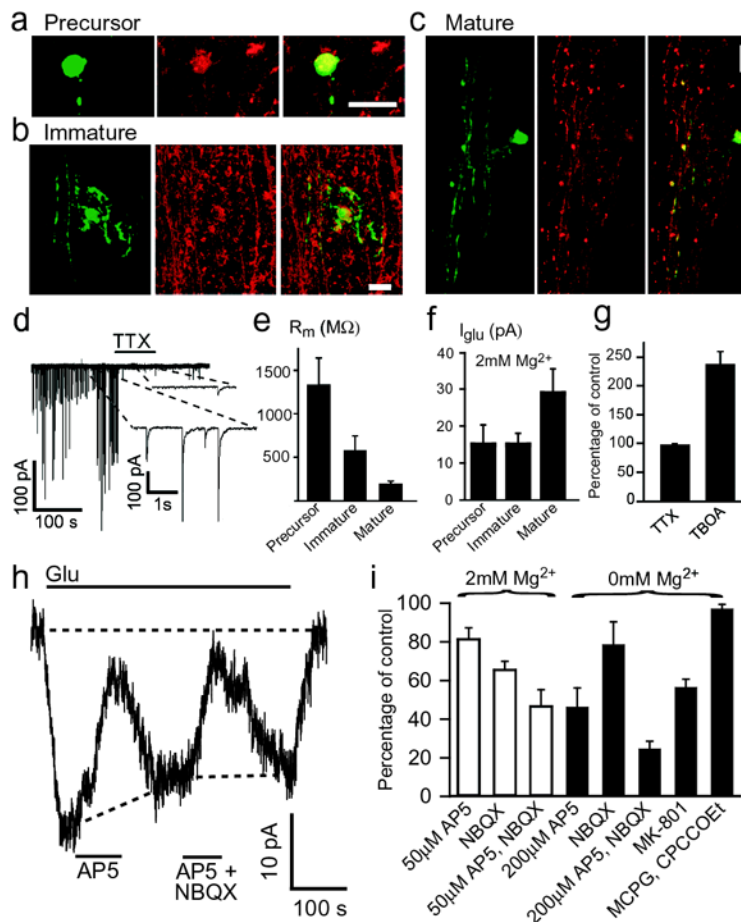


### Figure 1. Glutamate-evoked current in oligodendrocytes

**a-c** Lucifer (green) and antibody (red) to **(a)** NG2, **(b)** O4, and **(c)** MBP (colocalization in overlay, yellow). Scale 20  $\mu$ m. **d** TTX blocks synaptic currents in precursor. **e** Membrane resistance ( $\pm$ s.e.m.),  $p < 0.001$  comparing precursors with immature or mature. **f** Glutamate (100  $\mu$ M) evoked current ( $p = 0.11$  and  $0.14$  comparing 33 mature with 22 immature or 22 precursors). **g** Effect of TTX ( $n = 5$ ) and TBOA ( $n = 4$ ). **h** Effect of 200  $\mu$ M D-AP5 (blocks NMDA responses by  $\sim 78\%$ : Supplementary Material) and 25  $\mu$ M NBQX (blocks AMPA responses  $> 99\%$ ) in 0mM Mg. **i** Current remaining in 2mM  $Mg^{2+}$  ( $n = 7$ ) in 50  $\mu$ M AP5 ( $p = 0.02$ , blocks NMDA receptors by  $\sim 39\%$ ), 25  $\mu$ M NBQX ( $p = 0.0003$ ) and AP5+NBQX ( $p = 0.0008$ ), and in 0  $Mg^{2+}$  ( $n = 4-6$ ) in 200  $\mu$ M AP5 ( $p = 0.01$ ), 25  $\mu$ M NBQX ( $p = 0.16$ ), AP5+NBQX ( $p = 0.0003$ ), 10  $\mu$ M MK-801 ( $p = 0.002$ ) and 1mM MCPG plus 200  $\mu$ M CPCCOEt (mGluR blockers,  $p = 0.25$ ). All 2mM  $Mg^{2+}$  (except h,i),  $-63$ mV,  $24^\circ$ C.



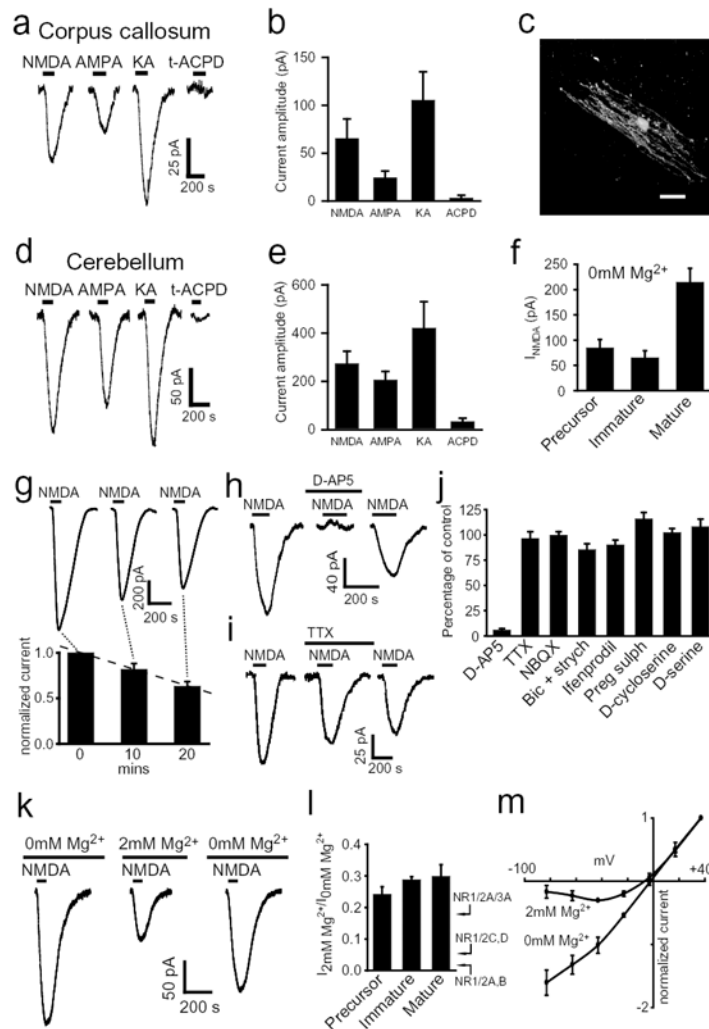


**Figure 2. Oligodendrocyte NMDA receptors show weak  $Mg^{2+}$ -block**

**a** Response of mature corpus callosum oligodendrocyte to  $60\mu M$  NMDA,  $20\mu M$  AMPA,  $30\mu M$  kainate (KA) and  $100\mu M$  trans-ACPD ( $0mM Mg^{2+}$ ). **b** Peak current in **a** for NMDA ( $n=22$  cells), AMPA ( $n=12$ ), KA ( $n=10$ ) and ACPD ( $n=5$ ). **c** Mature Lucifer-filled oligodendrocyte in corpus callosum (scale  $20\mu m$ ). **d** Responses of mature cerebellar oligodendrocyte in  $0mM Mg^{2+}$ . **e** Current in **d** for NMDA ( $n=26$ ), AMPA ( $n=23$ ), KA ( $n=5$ ) and ACPD ( $n=16$ ). **f** NMDA-evoked current in cerebellar cells ( $p=0.059$  and  $0.042$  comparing 79 mature with 19 immature or 26 precursors). **g** NMDA responses rundown linearly with time (dashed line) during repeated ( $1/10$  mins) applications: top, specimen cell; bottom, normalised data ( $n=10$ ). **h** Effect of D-AP5 ( $50\mu M$ ). **i** Effect of TTX ( $1\mu M$ ). **j** Effect of  $50\mu M$  D-AP5 ( $n=16$ ,  $p=10^{-18}$ ),  $1\mu M$  TTX ( $n=5$ ,  $p=0.64$ ),  $25\mu M$  NBQX ( $n=4$ ,  $p=0.96$ ),  $5\mu M$  strychnine plus  $20\mu M$  bicuculline ( $n=16$ ,  $p=0.14$ ), ifenprodil ( $10\mu M$ ,  $n=3$ ,  $p=0.18$ ), pregnenolone sulphate ( $100\mu M$ ,  $n=4$ ,  $p=0.085$ ), D-cycloserine ( $1mM$ ,  $n=3$ ,  $p=0.6$ ) and D-serine ( $100\mu M$ ,  $n=5$ ,  $p=0.34$ ) on NMDA-evoked current at  $-63mV$ . **k** NMDA response in  $0mM$ ,  $2mM$  and  $0mM Mg^{2+}$  again. **l** Fraction of NMDA-evoked current remaining in  $2mM Mg^{2+}$ , in 4 precursor, 6 immature and 9 mature cells (insignificantly different,  $p=0.51$ ). Arrows: values 22, 23 for NR1 with NR2C or 2D, 2A or 2B, or 2A and 3A. **m** Normalized I-V relation for NMDA-evoked current in two precursors in  $0mM$  and three different precursors in  $2mM Mg^{2+}$ . Cerebellum except a-c;  $0 Mg^{2+}$  (except k-m);

100 $\mu$ M glycine and 5 $\mu$ M strychnine (except D-cycloserine, D-serine in j); 60 $\mu$ M NMDA; 24°C, -63mV.

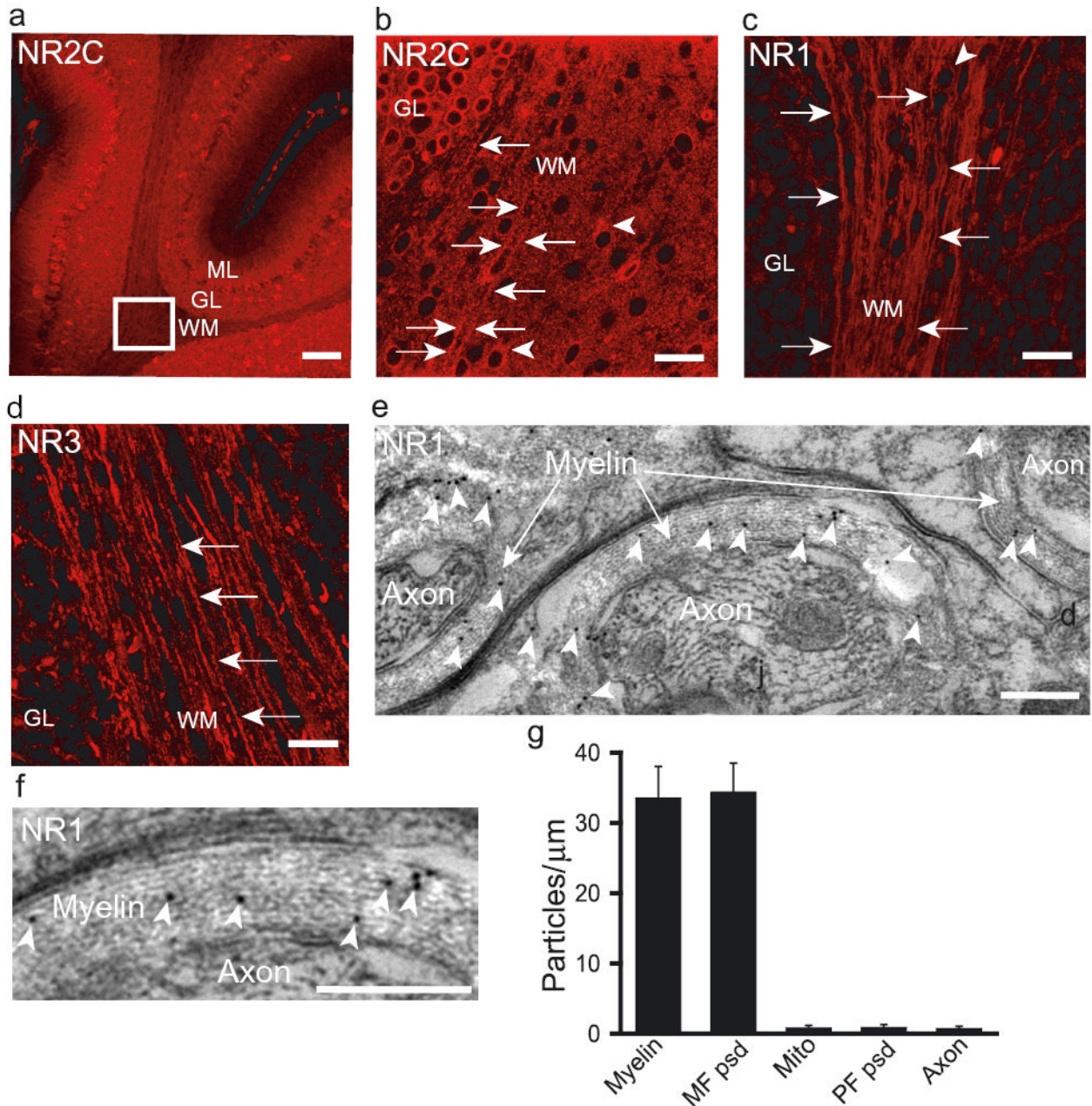


**Figure 3. Oligodendrocyte NMDA receptors**

**a** Cerebellar cortex labelled for NR2C (WM, white matter, GL granular layer, ML molecular layer). **b** Enlarged box in **a**. Arrows: oligodendrocyte process; arrow heads: oligodendrocyte soma. **c** Oligodendrocyte processes labelling with Chemicon NR1 antibody (see also Supplementary Fig. 6). **d** NR3 labelling. **e** Immunogold (black dots, arrowheads, Wenthold NR1 antibody) labelling cerebellar myelin. **f** Enlarged view of myelin. **g** Gold particle density over cerebellar myelin (17 sheaths), mossy fibre synapse (MF psd, n=20), parallel fibre-Purkinje synapse (PF psd, n=26), mitochondria in MF terminal (Mito, n=30), and axon cytoplasm (Axon, n=17). Scale bars: **a** 100 $\mu\text{m}$ , **b-d** 20 $\mu\text{m}$ , **e-f** 0.25 $\mu\text{m}$ .

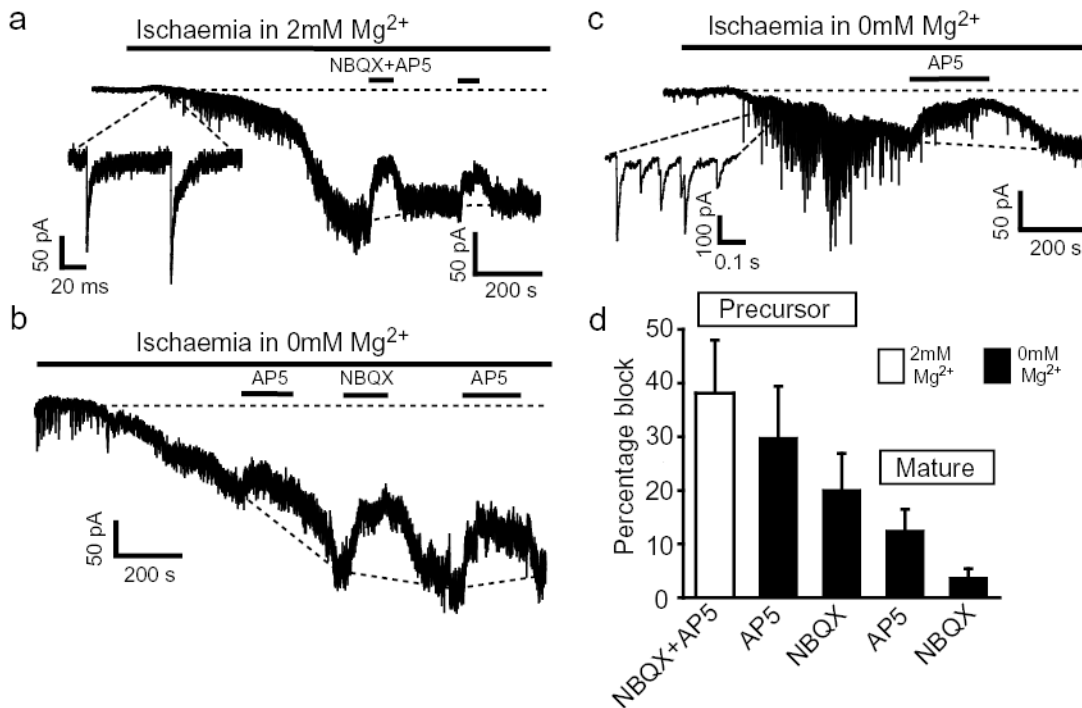


**Figure 4. Ischaemia activates NMDA receptors**

**a** Ischaemia-evoked current in precursor (2mM Mg<sup>2+</sup>) blocked by NBQX (25μM) plus D-AP5 (50μM) Inset: ischaemia-induced synaptic-like currents. **b** Precursor response to ischaemia (0mM Mg<sup>2+</sup>), blocked by D-AP5, NBQX. **c** Precursor response (0mM Mg<sup>2+</sup>) showing transient increase in synaptic currents, and most inward current blocked by D-AP5. **d** Fractional block of inward current: in 2mM Mg<sup>2+</sup> by D-AP5 plus NBQX in 7 precursors, and in 0mM Mg<sup>2+</sup> by D-AP5 or NBQX in precursors (9 for D-AP5, 7 for NBQX) and mature cells (9 for D-AP5, 10 for NBQX). P=0.098 comparing D-AP5 in precursors and mature cells; P=0.019 comparing NBQX in precursors and mature cells. All cerebellum, -63mV, 33°C.